Thermochimica Acta 498 (2010) 100–105

Contents lists available at ScienceDirect

Thermochimica Acta

journal homepage: www.elsevier.com/locate/tca

Adsorption properties of various forms of aluminium trifluoride investigated by *PulseTA®*

M. Feist, R. König, S. Bäßler, E. Kemnitz*

Institute of Chemistry, Humboldt University, Brook-Taylor-Strasse 2, D-12489 Berlin, Germany

ARTICLE INFO

Article history:
Received 6 August 2009
Received in revised form 2 October 2009
Accepted 11 October 2009
Available online 20 October 2009

Keywords:
Aluminium fluorides
Methanol adsorption
Pulse Thermal Analysis

ABSTRACT

The current study employs the Pulse Thermal Analysis (PTA) method to investigate the adsorption of gaseous methanol onto various forms of aluminium trifluoride drawing special attention to the strongly adsorbing β-AlF_3 and the recently described high-surface (HS) AlF_3. Simultaneously or subsequently occurring physisorption and chemisorption can be clearly distinguished and partly quantified. BET surface and NH_3-TPD data will be discussed together with the surface coverage by methanol determined by TA. The extraordinary sorptive properties of HS-AlF_3 are due to acidic sites at the remarkably large surface. The crystalline modifications η-AlF_3, θ-AlF_3, and κ-AlF_3 are less-important as they poorly adsorb exhibiting thermogravimetric curves without clearly expressed mass changes. Their surface loading is comparably poor as found for the stable modification α-AlF_3.

1. Introduction

During the last two decades, numerous studies were devoted to aluminium fluoride in various crystalline and amorphous modifications as to aluminium-based hydroxyfluorides. The scientific interest is primarily explained by the attempts to improve and to understand the catalytic properties of these substances, but by special applications as well, e.g. such as thin coatings. The studies led to the design of novel preparation routes, e.g. a sol–gel process yielding nano-sized, mesoporous high-surface aluminium fluoride (HS-AlF_3) [1,2], microwave-assisted hydrothermal synthesis [3,4], or mechanochemical activation by high-energy ball milling [5,6]. Meanwhile, magnesium fluoride, being analogously sol–gel prepared as HS-AlF_3, can be deposited on glassy surfaces forming stable transparent thin films exhibiting extraordinary optical and protective properties [7].

HS-AlF_3 and related phases were the subjects of a series of structural, chemical, and computational studies [8–10] which allowed to conclude that the enormous Lewis acidity being comparable to that of SbF_5 [11] is responsible for the extraordinary properties.

Exemplarily, HS-AlF_3 catalyzes the isomerisation of 1,2-dibromohexafluoropropane to 2,2-dibromohexafluoropropane, which is catalyzed only by the strongest Lewis acids known [12]. So far, several techniques were applied to characterize and compare the strength of the Lewis acidic centres of HS-AlF_3 and related phases, including pyridine photoacoustic IR [12,13], NH_3-TPD [1,13] or IR spectroscopy of adsorbed CO molecules [8].

The present study will contribute to the knowledge of the sorption properties of the mentioned aluminium fluoride phases by applying a promising tool in adsorption studies, i.e. the *Pulse Thermal Analysis®* [14–16].

2. Experimental

2.1. Synthesis

Seven different modifications and specially prepared forms of AlF_3 have been synthesized (Table 1). The substances were pure and did not contain amorphous parts as proved by their X-ray powder diffractograms combined with a detailed spectroscopic study of the phases by employing ^{27}Al and ^{19}F solid state MAS NMR, XPS and IR spectroscopy. These results will be reported elsewhere [17].

α-AlF_3 was used as commercially available (Aldrich) or prepared by thermal decomposition of $(NH_4)_3[AlF_6]$ in a nitrogen flow at 700 °C. A typical experiment started from 3 g $(NH_4)_3[AlF_6]$; (3 h tempering, cooling down in nitrogen; XRD: PDF 44-231) [18].

β-AlF_3 was obtained by thermal decomposition of α-$AlF_3 \cdot 3H_2O$ [(PDF: 43-436; to be carefully distinguished from β-$AlF_3 \cdot 3H_2O$ (PDF: 35-872)]. A first reaction step consists in heating the educt in a Schlenk tube in vacuum at 200 °C. The second step is re-heating the intermediate tightly packed in an aluminium foil ("self-generated atmosphere") in a tube oven at the same 200 °C in a nitrogen flow, followed by a tempering step at 400 °C (1 h). The sample is cooled down under nitrogen [18,19].

* Corresponding author. Tel.: +49 30 2093 7555; fax: +49 30 2093 7277.
E-mail addresses: feistm@chemie.hu-berlin.de (M. Feist), koenigre@chemie.hu-berlin.de (R. König), sigrid.baessler@chemie.hu-berlin.de (S. Bäßler), erhard.kemnitz@chemie.hu-berlin.de (E. Kemnitz).

0040-6031/$ – see front matter © 2009 Elsevier B.V. All rights reserved.
doi:10.1016/j.tca.2009.10.008

Table 1
Structural and surfacial characterization for various forms of AlF_3.

	Structure type	Ref.	Structural features	S_{BET}[a] [m²/g]	m_{sample} [mg]	n_{MeOH}[b]			n_{NH_3}[c]	
						[μmol/g]	[mol%]	[μmol/m²]	[μmol/g]	[μmol/m²]
α-AlF_3	VF_3 (LT)	[27]	3D network	3	31.48	0	0	0	–	–
β-AlF_3	HTB	[19]	Hexagonal channels	31	43.81	107	0.9	3.5	380	12.2
β-AlF_3 *gel*	HTB	[22]	Hexagonal channels	43	14.04	221	1.8	5.1	130	3.0
η-AlF_3	Pyrochlore	[18,21]	Channels	2	36.68	8	0.07	4.0	160	80
κ-AlF_3	TTB	[21]	Tetra/pentagonal channels	19	17.64	91	0.76	4.8	–	–
θ-AlF_3	Own type	[20,29]	3D network	64	26.44	0	0	0	240	3.8
HS-AlF_3	Amorphous	[1,2]	Mesoporous	250	12.80	1090	7.7	4.0	900	3.6

[a] BET surface [31].
[b] Surface loading with methanol from PTA experiments related to m_S.
[c] NH_3-TPD (cf. [28] and Section 2).

θ-AlF_3 is formed in a two-step decomposition reaction in vacuum at 450 °C starting from $[N(CH_3)_4]AlF_4{\cdot}H_2O$ [20]. A typical experimental setup is: 2 g educt, open corundum crucible in a Quartz tube, evacuation with a membrane pump, tempering for 1 h; cooling down at normal air (XRD: PDF 47-1659).

η-AlF_3 has been characterized first by Herron et al. [21]. A comparably simple synthesis route has been described by Krahl: X-ray amorphous aluminium chloride fluoride (ACF) is thermally decomposed in a dynamic vacuum at 450 °C [18].

κ-AlF_3 was prepared according to Herron et al. [21] following the three-step synthesis route passing $PyHAlF_4$ and β-NH_4AlF_4 as isolable intermediates.

The gel form of β-AlF_3 has been synthesized by supercritical drying at 300 °C in an autoclave starting from a $\{AlF_{3-x}(OiPr)_x/i$-PrOH} gel (cf. [1,2]) and MeOH. The autoclave was depressurized at the same temperature. An extremely voluminous aerogel-like material with a BET surface between 40 and 66 m²/g was obtained [22].

The methanol used for the liquid injections was dried by common techniques, distilled, and stored over pre-dried molecular sieve A4 under nitrogen.

2.2. Thermal analysis

The *PulseThermalAnalysis*® (PTA) experiments have been performed using a NETZSCH thermoanalyzer STA 409 C *Skimmer*® system, equipped with a BALZERS QMG 421, enabling *on line*-coupled TA-MS measurements, and a commercial PTA box. The self-made liquid injection unit comprises a heated (120 °C), septum-tightened GC injector implemented in the heated stainless steel tube of the gas supply system. It is placed between the PTA box and the thermobalance. A microliter GC syringe is used. The dead time between injection and detection amounted to 60–70 s for the given flow conditions. The thermoanalytical curves (T, DTA, TG and DTG) have been recorded together with the ionic current (IC) curves in the multiple ion detection (MID) mode [14,15]. A DTA–TG sample carrier system with platinum crucibles (baker, 0.8 ml) and Pt/PtRh10 thermocouples was used. Samples of 25–40 mg each were measured versus empty reference crucible. A constant purge gas flow of 70 ml/min N_2 5.0 (MESSER-GRIESHEIM), a constant heating rate of 10 K/min or a isothermal regime with T_{iso} = 46–48 °C was applied. The raw data have been evaluated utilizing the manufacturer's software PROTEUS® (v. 4.3) and QUADSTAR® 422 (v. 6.02) without further data treatment, e.g. such as smoothing.

2.3. Surface determination

A Micromeritics ASAP 2010 apparatus has been used to record the N_2 adsorption isotherms at 77 K. Prior to each measurement, the samples were degassed at 4×10^{-3} Torr and 200 °C for 10 h. The surface area was calculated according to the BET method.

2.4. Temperature-programmed ammonia desorption (NH_3-TPD)

The samples were pretreated at 250–300 °C for 1 h. Afterwards, ammonia was adsorbed onto the surface at 393 K. Ammonia desorption was monitored upon heating (10 K/min up to 773 K) by FTIR detection of the band at 930 cm^{-1} (FTIR system 2000, PerkinElmer). The total amount of ammonia desorbed was determined volumetrically (excess of H_2SO_4, back-titration with NaOH solution [28].

3. Methodology and results

3.1. The PulseTA® method

The adsorption ability of solids can be studied by utilizing the *PulseTA*® (PTA) technique. It is a promising tool in thermal analysis [14–16] and has been successfully applied to the solid state chemistry of fluorides [23,24]. The PTA technique is normally used for the quantitative interpretation of TA-MS or TA-FTIR curves based on a preceding calibration of the ion current (IC) or IR signals [14,15]. The potential of PTA by quantitative signal evaluation is impressing in the case of capillary-coupled TA-MS devices, but limited in the case of skimmer systems which is due to its constructive design [25,26]. A PTA apparatus can also be utilized in terms of a "catalytic reactor" allowing for the injection of one or two gases onto a sample subjected to a controlled heating program [23]. Low-boiling liquids and even aqueous HF [24] can be injected as well (see Section 2). A typical PTA experiment in the field of catalytically active oxides or fluorides, which often contain surfacially adsorbed water and/or OH groups, comprises the following sequence of steps performed with one single sample:

(1) Pretreatment by heating in the appropriate carrier gas (preferably inert such as nitrogen) up to the chosen adsorption temperature to be studied.
(2) Cooling down to room temperature.
(3) Starting the measuring run (i.e. constantly heating or setting an appropriate isothermal temperature level).
(4) Injection of gas (typically 250–500 μL) or liquid pulses (1–5 μL) during heating or at the chosen isothermal plateau and recording of the TA-MS curves with appropriate mass numbers in the MID mode.
(5) Desorption (i.e. further heating or re-heating after cooling down to 25 °C).

Typical experimental curves according to steps (1), (4), and (5) are presented in Figs. 5–7, respectively.

3.2. Blank experiments for studying the methanol adsorption

In order to design a blank experiment that should precede a PTA measurement one has to consider three aspects: (1) a possible

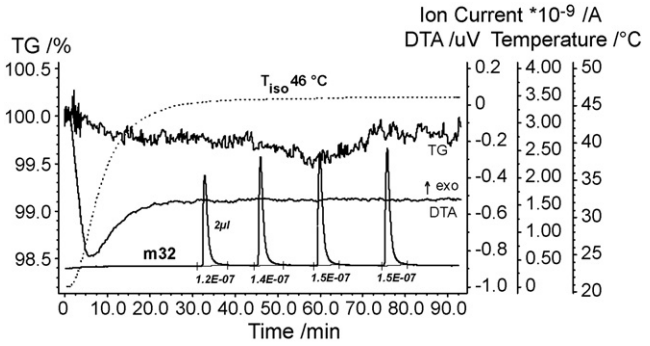

Fig. 1. TA-MS curves for preparing a *PulseTA*® experiment. Four injections of 2 μL liquid methanol in the recipient, isothermally held at 46 °C, without a sample are represented by the IC signals for the mass number m32 (CH_3OH^+) together with the integral intensities (in A s). Neither a DTA effect nor a detectable mass gain can be detected.

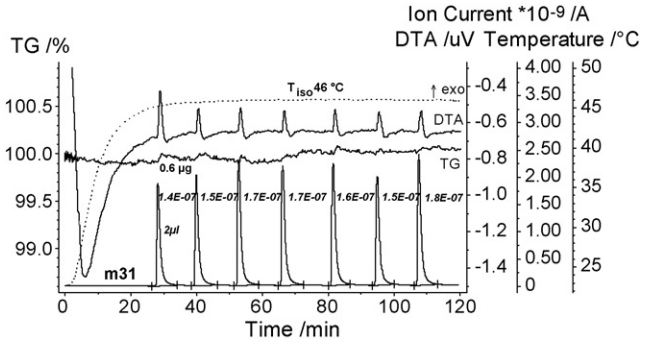

Fig. 2. TA-MS curves for a *PulseTA*® experiment on pre-heated (250 °C in N_2) α-AlF_3 (31.48 mg) in nitrogen with the IC curve for the mass number m31 (CH_3O^+) representing the methanol injections.

enthalpic effect of injecting pulses of gaseous methanol into the carrier gas stream must be known; (2) the evolution of the peak areas of the IC curves to be followed ($m/z = 31$[1] or 32 in this case) must be known for the case of injecting into the apparatus with empty crucibles; (3) it is further important to know the behaviour of an inactive compound under the chosen experimental conditions. For the present study of various modifications of aluminium fluorides, a well-crystalline α-AlF_3 seemed to be the typical representative of an inactive compound as it is known not to act as Lewis acid catalyst [13].

3.2.1. Injection into an empty apparatus

As can be seen in Fig. 1, no enthalpic effect can be detected that could be attributed to a mixing effect of the evaporated methanol in the carrier gas.

The IC area of the first pulse is somewhat smaller than the following ones. As no mass gain corresponds to the pulse, obviously a certain fraction of the injected methanol is adsorbed at the inner surface of the measuring cell. This is not surprising as the recipient has been evacuated during the measurement preparation.

3.2.2. Injections onto α-AlF_3

Fig. 2 demonstrates that the original assumption concerning the inactivity of α-AlF_3 cannot be confirmed. It shows, in contrast, weak methanol adsorption predominantly as physisorption. Only the first injection pulse (2 μL each) causes a very small mass gain of 0.6 μg that practically disappears over the experiment time of 120 min. All DTA signals exhibit the characteristic form of a sharp exothermal effect indicating physisorption that is immediately followed by the broader endothermal effect being due to desorption by the continuous gas flow of the carrier gas (see below).

Again, the IC peak area of the first pulse is smaller than that of the following ones; their areas are almost constant within the experimental error. The area variation reflects the volume error that is greater for the manual injection of liquids using a μL-syringe than for the injection of permanent gases by an injection loop contained in the commercially available PTA box.

3.3. The sorption behaviour of β-AlF_3

3.3.1. Adsorption of methanol

The findings reported before enabled us to perform analogous sorption experiments with β-AlF_3, a phase expected to adsorb much stronger than α-AlF_3. A sample of 44.29 mg has been pretreated by heating in vacuum for 2 h at 250 °C which lead to a water release of 0.48 mg (1.08%). The remaining solid (43.81 mg), which was then cooled down under nitrogen, provided a "fresh" surface ready to be loaded with the adsorbate.

As shown in Fig. 3, four pulses of 3 μL liquid methanol are sufficient for saturating the surface of β-AlF_3. Only the TG step for the first pulse indicates chemisorption alone (70 μg). The following three pulses show the overlapping of chemisorption by an increasing portion of physisorption. The initial mass gain at each injection peak, caused by the methanol sorption, is afterwards reduced due to the release of physisorbed methanol into the carrier gas stream. The fifth injection peak already (not monitored) affects no mass gain any more.

The remaining net mass gain for the second to fourth steps (50, 20 and 10 μg) represents the chemisorbed part of methanol. With the total mass gain of 150 μg for the entire experiment one calculates a surface loading of 0.107 mmol/g (0.9 mol%) CH_3OH.

It is noteworthy that both the qualitative interpretation of the TG curve shape presented here and the quantitative determination of the surface loading exactly correspond to the procedure proposed for ZSM-5 zeolites [16]. Moreover, not only the TG curve, but the DTA traces as well give a good insight in details of the sorption behaviour. This is especially remarkable as, usually, the sensitivity of TG data is considered to be almost one order of magnitude better than that of DTA information. However, a careful inspection of the DTA traces illustrates as well fine details of the sorption processes, e.g. the different behaviour during the first and the following pulses as well as differences in the heat exchange. So the first pulse in Fig. 3, representing chemisorption alone, causes only a sharp exothermal DTA signal. If desorption of physisorbed molecules begins to occur

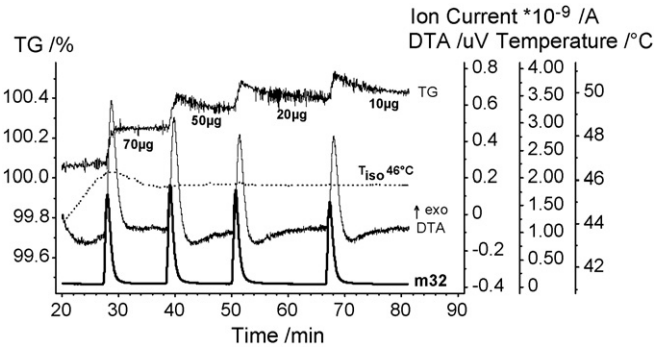

Fig. 3. TA-MS curves for a *PulseTA*® experiment on pretreated (2 h, 250 °C; vacuum) β-AlF_3 (43.81 mg, $\Delta m = +150$ μg) in nitrogen with the IC curve for the mass number m32 (CH_3OH^+).

[1] The labelling of mass numbers, e.g. $m/z = 31$, will be shortened in the following as m31.

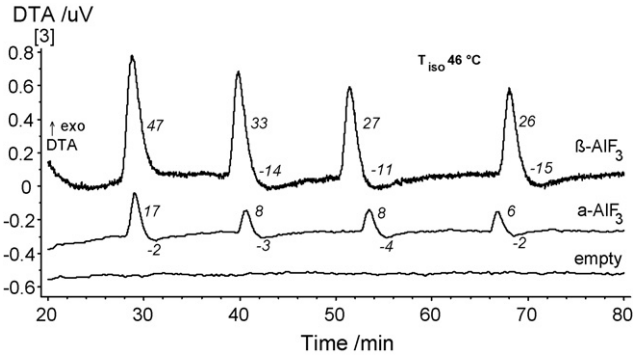

Fig. 4. DTA curves for the first four injection pulses of methanol onto α- and β-AlF_3 and without a sample (from Figs. 1–3). The peak areas (μV s) are standardized to equal injection volumina.

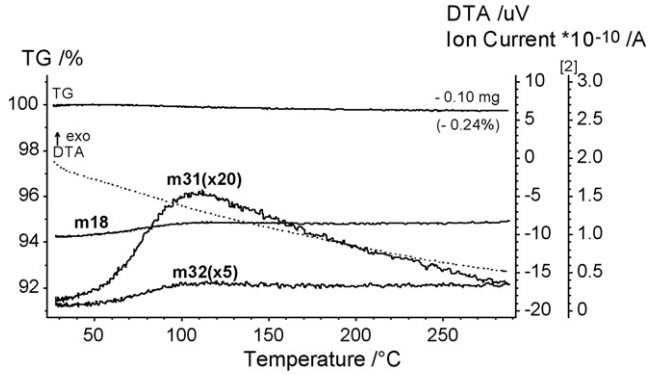

Fig. 5. TA-MS curves for the desorption of methanol from β-AlF_3 loaded in a preceding PTA experiment (cf. Fig. 3) after cooling down under nitrogen. The mass numbers m18 (H_2O^+), m31 (CH_3O^+), and m32 (CH_3OH^+) are shown (if more than one mass number is depicted, the scaling for the IC given in the plot corresponds to the most intensive mass number, i.e. mostly that for water, m18).

(cf. the TG curve shape), the endothermal desorption affects the broad signal that follows the strong exothermal peak. As expected, the peak area for chemisorption is considerably greater than for physisorption which can be deduced from the decreasing area values for the exothermal peaks for β-AlF_3[2] as shown by the comparison in Fig. 4. By subtracting the area values for physisorption alone from the sum value (cf. β-AlF_3 in Fig. 4), one can separate the net exothermicity for the chemisorption at the given surface (but see below).

A further detail is noteworthy. For the case of pure physisorption, where no net mass gain persists (α-AlF_3 in Fig. 4), one could have expected that the peak areas of exothermal physisorption and endothermal desorption should be approximately equal as the processes are reversible and no further enthalpic contribution should appear. This is not the case, as clearly expressed for α-AlF_3 (6–8 μV s for the adsorption vs. 2–4 μV s for the desorption). Here, one should bear in mind that both processes are competitive and partly overlap each other with a differing time dependence. Hence, it is impossible to clearly separate the individual part of each contribution and the peak areas are necessarily different. This is a limitation also for the above-mentioned area subtraction when trying to separate quantitatively the portion of chemisorption.

To summarize, one should note that Fig. 4 illustrates qualitatively and quantitatively that α- and β-AlF_3 behave differently. Only the empty apparatus yields a real blank experiment whereas α-AlF_3, unlike expected, is a weak adsorbent showing predominantly physisorption. β-AlF_3, however, exhibits both chemi- and physisorption and adsorbs strongly.

3.3.2. Different desorption behaviour

The adsorption of methanol is not completely reversible. If the loaded sample of β-AlF_3 as presented in Fig. 3 is re-heated under nitrogen in a subsequent TA run, 71% (0.10 mg) of the originally adsorbed 0.15 mg methanol was released from the surface (Fig. 5). The desorption starts at about 50 °C, i.e. only slightly higher than the loading temperature 46 °C and is spread over a wide temperature range (50–200 °C) with a desorption maximum at 110 °C. As indicated by the IC curve for m18, a minor co-adsorption of water during the preceding methanol injections cannot be fully excluded.

Another result is obtained when a methanol-loaded β-AlF_3 (0.12 mg on 25.86 mg AlF_3; 1.23 mol% MeOH) is stored 24 h at humid air. In this case, no desorption of methanol at all can be detected under re-heating (curves not shown here). It is completely substituted by water (0.14 mg; 2.43 mol% H_2O), which is released between 50 and 200 °C with an IC maximum for m18 around 100 °C.

The observation that a certain part of the adsorbed methanol is retained at the surface needs an interpretation. It cannot be related to the channels existing in the HTB structure of β-AlF_3 as the methanol molecule is too large to get inside the channels.

3.4. The sorption behaviour of HS-AlF_3

The sequence of Figs. 6–8 represents the adsorption study of HS-AlF_3. The mass loss occurring during the thermal pretreatment is greater (5.36%) than for the other AlF_3 modifications investigated

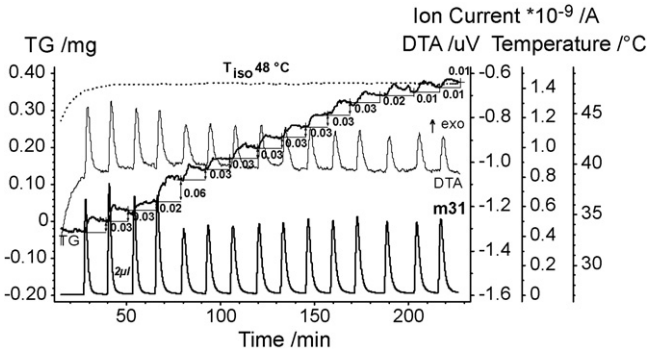

Fig. 6. PTA curves of pretreated (250 °C; N_2) HS-AlF_3 (12.8 mg, Δm = +0.41 mg).

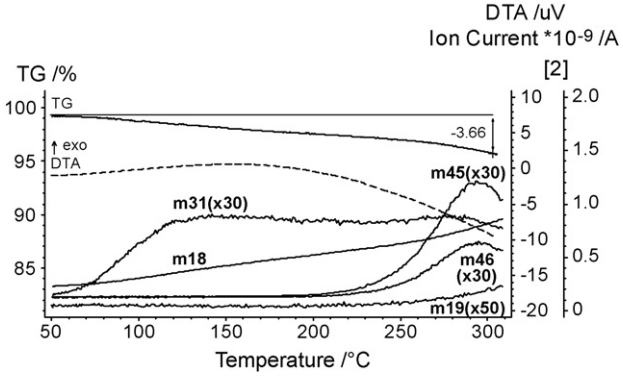

Fig. 7. TA-MS curves for the desorption of methanol from HS-AlF_3 (13.21 mg, Δm = −0.48 mg) precedingly loaded with 0.41 mg MeOH (cf. Fig. 6). Note the coincidence of the weakly expressed second IC maximum for m31 above 250 °C with the IC maxima for m45$(M-1)^+$ and m46(M^+) caused by dimethylether.

[2] Note that the area values for the desorption peaks (between −11 and −15 μV s for β-AlF_3 or −2 and −4 μV s for α-AlF_3, cf. Fig. 4), have to be considered each as practically constant within the experimental error.

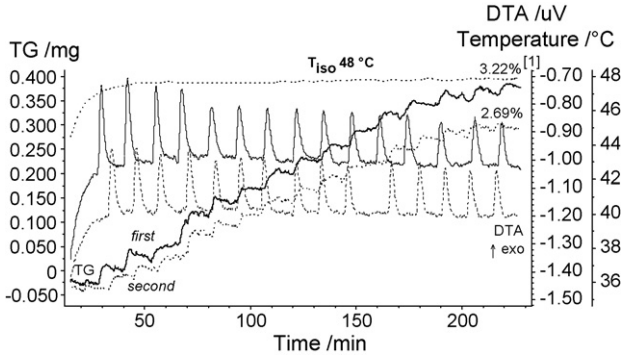

Fig. 8. Comparison of the PTA curves for the first and the second adsorption measurements of pretreated (250 °C; N_2) HS-AlF_3.

which is an expression of the strong sorption activity of HS-AlF_3. As the sample was glove box-stored and -weighed, the water uptake occurs exclusively during the opening of the measuring cell and the positioning of the TA crucible onto the sample holder (60–70 s on humid air). Interestingly enough, this did not lead to an observable pyrohydrolysis of the fluoride as proved by the course of the mass numbers 19 and 20 (not shown here).

As can be seen in Fig. 6, the adsorption behaviour of HS-AlF_3 is qualitatively and quantitatively quite different from all the other modifications studied here. Firstly, the absolute methanol uptake is impressing: 1.19 mmol/g (7.7 mol%) which is more than 5 times greater than for the comparably strongly adsorbing β-AlF_3 gel (Table 1). Moreover, the TG curve shape shows that the adsorption becomes weaker with the 13th to 15th injection pulses, but is not yet definitely finished. Secondly, the exothermal DTA peaks for the injections are not followed by the above-mentioned (Section 3.3.1) weak endothermal post-effects indicating the desorption of physisorbed species in the gas flow. This means that exclusively chemisorption occurs in the case of HS-AlF_3! This is in line with the TG curve shape, even if the individual steps are not as ideally expressed as observed for β-AlF_3 (cf. Fig. 3), where the distinction between chemi- and physisorption is extraordinarily clear.

Not only the adsorption behaviour, but the desorption behaviour of HS-AlF_3 as well is different from all other modifications investigated. The IC curves in Fig. 7 to be compared with Fig. 5 demonstrate that the desorbed amount is within the experimental error identical with the precedingly uptaken amount (0.41 mg vs. 0.48 mg). This is not generally the case for the other AlF_3 modifications. Only methanol is released in the usual desorption range (50–250 °C), a water release can be detected only above 250 °C and is attributed to beginning pyrohydrolysis (see below). The desorption profile is spread over a broader temperature interval up to 230 °C and the first maximum is shifted to higher temperatures (130 °C). A weakly expressed second intensity maximum for m31 appears at about 280 °C. Moreover, the m18 and m19 intensities begin to increase. This can be explained by the formation of dimethylether from methanol which is catalyzed by HS-AlF_3 and which produces water as the second product. As a consequence, HF is released due to the beginning pyrohydrolysis (m19). This behaviour is comparable to that observed for the precursors of HS-AlF_3 [12], where ether formation was established during the post-fluorination yielding the final HS-AlF_3 and where the di-*i*-propylether originates from the *i*-propoxide groups contained in the precursor phase.

The almost reversible adsorption of methanol which has been deduced from the findings for the first loading described above implicated the question of the repeatability of the surface loading of HS-AlF_3. As can be seen in Fig. 8, the methanol adsorption is reversible, but in a limited manner. Interestingly enough, the qualitative character of exclusively chemisorption does not change. The absolute methanol uptake, however, is lower (2.69% vs. 3.22%). Here as well, the methanol adsorption is not finished with the 15th pulse. The desorption after the second loading (not shown here) is as complete as the first one (0.33 mg uptake vs. 0.31 mg loss).

If water is adsorbed, the behaviour is different. After pure chemisorption at the beginning of the experiment, one observes physisorption starting with the sixth injection pulse (of nine in total) and the adsorption reaches saturation. The total mass gain amounts to 1.63%, i.e. 3.8 mol% H_2O. Even if this is only the half of the methanol loading, a value of 3.8 mol%, nevertheless, indicates a good sorption behaviour.

3.5. The adsorption behaviour of further modifications of AlF_3

Four further AlF_3 phases have been investigated in the same way: a gel-like form of β-AlF_3, prepared via a special sol–gel synthesis route [22] to give an especially large surface, and, finally, η-AlF_3, θ-AlF_3, and κ-AlF_3, all representing crystalline modifications (cf. Table 1).

As expected, the gel-like form of β-AlF_3 showed a strong adsorption of methanol and the value of 0.2 mmol/g (1.6 mol%) surface loading, being twice as much than for normal β-AlF_3 (0.9 mol%), is noteworthy. On the other hand, this is only 22% of the adsorption capacity of HS-AlF_3.

η-AlF_3 exhibited a distinctly differing sorption behaviour. Only the first pulse yields a clear picture indicating exclusively chemisorption without any endothermicity after the exothermal adsorption peak. Starting with the second injection already, an unstable course of the TG curve was recorded. Adsorption and desorption seem to alternate in an irregular manner. A net mass gain of 10 μg persists which leads to a very low surface loading of 0.008 mmol/g (0.07 mol%). This is in the same order of magnitude as observed for α-AlF_3, where practically no persisting adsorption could be established.

More or less identical findings have been obtained both for κ-AlF_3 and θ-AlF_3. They show nearly the same sorption features, i.e. a less-regular course of the TG curves: certain pulses do not effect a detectable mass gain, certain others even show a slight mass loss. Roughly, the three modifications η-AlF_3, κ-AlF_3, and θ-AlF_3 behave in the same way as does α-AlF_3.

3.6. Discussion

A comprehensive overview about the sorption properties is given in Table 1. The values for the surface loading are compared with those for the NH_3-TPD, directly representing the sum of Lewis and Brønsted acid centres, and with the BET surface values. The BET surfaces of four modifications are relatively close together, except the three extreme values, i.e. the very small surface areas of α- and η-AlF_3 and the very high surface of HS-AlF_3. As the NH_3-TPD data represent the ammonia amount thermally removed from the covered surface, the values given in μmol NH_3/m^2 have to be understood as μmol acid centres/m^2.

Differently from NH_3, which easily can act as Lewis or Brønsted base, CH_3OH should only behave as a Lewis base probing exclusively the Lewis acidic centres.

However, since the fluorides are pretreated at 250 °C, the absolute amount of Brønsted acidic centres determined by NH_3-TPD is negligible in this case. Based on the assumption that the values for the amount of centres on the surface calculated by the methods of TPD and of PTA represent the part of the interaction of Lewis acidic centres and the probe molecules (TPD: NH_3, PTA: CH_3OH), the values should be directly comparable.

Unambiguously, the starting point for an interpretation of the experimental and calculated data regrouped in Table 1 must be, on

the one hand, the interplay of acidic sites and porosity, and, on the other hand, structural aspects such as the channel structure of certain AlF_3 modifications together with the size and the coordinative situation of surfacial AlF_6 units. It can be stated that the evolution of the values for S_{BET}, n_{MeOH} in μmol/g and in mol% is qualitatively almost identical, except the non-adsorbing α- and θ-AlF_3. All these data are mass-based. If the surface loading by methanol is related, however, to the actual surface basing on S_{BET}, the practical identity of all calculated values given in μmol MeOH/m^2 might surprise. This is especially true if they are compared with the surface-related values (in μmol NH_3/m^2) obtained with the NH_3-TPD method. Reconsidering, however, the different size of the probe molecules (NH_3 would fit into the channels of β- or η-AlF_3, whereas CH_3OH is too large), the values obtained by NH_3-TPD are possibly overestimated. An uptake of small molecules into the channels as recently observed for water and HTB tungstates [30] seems to play a role also for the adsorption of NH_3 onto β- and η-AlF_3 resulting in higher surface-related values for these phases (Table 1, last column). Taking further into account that MeOH, unlike NH_3, interacts exclusively with Lewis acidic centres, the analytical information obtainable by MeOH-PTA seems to be more specific.

Concerning the values obtained with the MeOH-PTA experiments, one has further to bear in mind, that the geometric and coordinative situation of the AlF_6 octahedra, being the basic structural unit of all AlF_3 modifications, is not so strongly different from each other, even if they adopt different crystal structures or amorphous forms. Interpreting the calculated values for the fluorides, the surface area and the morphology of the investigated phase is clearly one of the biggest influencing variables governing the adsorption properties and therewith the amount of offered acidic centres. Additionally, the particular Lewis acidic behaviour of β-AlF_3 and HS-AlF_3, one of the strongest solid Lewis acids known, can be proved by the extraordinary adsorption behaviour of MeOH.

The variations of distortions and linking of the AlF_6 octahedra, which make the main differences (among them the channel feature) between the different crystalline modifications, seem to exhibit only a minor effect. Nevertheless, the structural variations which, on the other hand, are clearly to be identified by XRD or other structural methods such as NMR of various nuclei [17] are at least responsible for subtle differences, e.g. as shown for the characteristics of β-AlF_3, which shows Lewis acidic behaviour in comparison to the other crystalline fluorides, such as κ- or η-AlF_3 both exhibiting channel structures.

This might explain that the undoubtedly extraordinary position of HS-AlF_3 in the sequence of phases investigated is not expressed in a comparably extraordinary value for the methanol loading given in μmol/m^2. If, however, the loading is regarded mass-based, the situation is unambiguous. This can be regarded as a hint for the great potential of the PTA method and would be a further demonstration of the deep insight in fine details of the sorption process itself, which is obtainable by employing PTA. NH_3-TPD, being well-established in catalysis research, yields a quantitative information about the surface coverage and is completed by the qualitative description deducable from the desorption profile. PTA, on the other hand, not only yields quantitative data via enthalpy and mass changes (the latter often being underestimated in catalysis papers), but also allows to distinguish between different kinds of adsorption, and even to inject pulses of various liquids or gases onto a solid in one single carefully designed experiment. This might be considered as a "titration" of the surfaces.

4. Conclusions

Summarizing the reported observations it is concluded that the methanol adsorption behaviour of the various forms of AlF_3 is not governed by an influence of the structure, e.g. by the existence of channel structures, but exclusively by surface effects, i.e. primarily by Lewis acid sites and the size and the morphology of the phase particles.

It could be demonstrated that PTA, indeed, is a valuable tool for investigating the sorption properties of solids which allows to follow and to visualize fine details of the interaction, i.e. the energetic balance and the mass changes as well. But these quantitative aspects (enthalpy and mass) are, at least for this group of AlF_3 polymorphs, better understood than the interplay of acid sites and porosity, on the one hand, and structural aspects such as the channel structure of certain AlF_3 modifications on the other hand. Comparing the information that could be obtained here from NH_3-TPD with that deduced from PTA experiments, the latter seems to differentiate remarkably better in the case of the investigated AlF_3 modifications.

Acknowledgements

Dr. Ekkehard Füglein (Netzsch Gerätebau GmbH, Selb, Germany) and Dr. Jan Hanss (University of Augsburg, Germany) contributed to the presented work by supporting us for the area integrations of the DTA curves in Fig. 4 (E.F.) and by helpful trilateral discussions of experimental details. This is gratefully acknowledged.

References

[1] E. Kemnitz, U. Groß, St. Rüdiger, Ch. Shekar, Angew. Chem. Int. Ed. 42 (2003) 4251–4254.
[2] St. Rüdiger, E. Kemnitz, Dalton Trans. (2008) 1117–1127.
[3] D. Dambournet, A. Demourgues, C. Martineau, S. Pechev, J. Lhoste, J. Majimel, A. Vimont, J.-C. Lavalley, C. Legein, J.-Y. Buzaré, F. Fayon, A. Tressaud, Chem. Mater. 20 (2008) 1459–1469.
[4] M. Gaudon, J. Majimel, J.-M. Heintz, M. Feist, D. Dambournet, A. Tressaud, J. Fluorine Chem. 129 (2008) 1173–1179.
[5] G. Scholz, M. Feist, E. Kemnitz, J. Solid State Sci. 10 (2008) 1640–1650.
[6] G. Scholz, R. König, J. Petersen, B. Angelow, I. Dörfel, E. Kemnitz, Chem. Mater. 20 (2008) 5406–5413.
[7] H. Krüger, E. Kemnitz, A. Hertwig, U. Beck, Thin Solid Films 516 (2008) 4175–4177.
[8] Th. Krahl, A. Vimont, G. Eltanany, M. Daturi, E. Kemnitz, J. Phys. Chem. C 111 (2007) 18317–18325.
[9] E.K.L.Y. Hajime, J.L. Delattre, A.M. Stacy, Chem. Mater. 19 (2007) 894.
[10] A. Wander, C.L. Bailey, S. Mukhopadhyay, B.G. Searle, N.M. Harrison, J. Mater. Chem. 16 (2006) 1906.
[11] K.O. Christe, D.A. Dixon, D. McLemore, W.W. Wilson, J.A. Sheey, J.A. Boatz, J. Fluorine Chem. 101 (2000) 151.
[12] S. Rüdiger, U. Groß, M. Feist, H.A. Prescott, C.S. Shekar, S.I. Troyanov, E. Kemnitz, J. Mater. Chem. 15 (2005) 588–597.
[13] A. Hess, E. Kemnitz, J. Catal. 149 (1994) 449–457.
[14] M. Maciejewski, C.A. Müller, R. Tschan, W.-D. Emmerich, A. Baiker, Thermochim. Acta 295 (1997) 167.
[15] M. Maciejewski, A. Baiker, Thermochim. Acta 295 (1997) 95.
[16] F. Eigenmann, M. Maciejewski, A. Baiker, Thermochim. Acta 6276 (2000) 1.
[17] R. König, G. Scholz, K. Scheurell, D. Heidemann, I. Buchem, W.E.S. Unger, E. Kemnitz, J. Fluorine Chem. (in press).
[18] T. Krahl, Dissertation, Humboldt-Universität zu Berlin, 2005.
[19] D.L. Xu, Y.Q. Luo, Y. Li, L.B. Zhou, W.K. Gai, Thermochim. Acta 352 (2000) 47–52.
[20] A. Le Bail, J.L. Fourquet, U. Bentrup, J. Solid State Chem. 100 (1992) 151–159.
[21] N. Herron, D.L. Thorn, R.L. Harlow, G.A. Jones, J.B. Parise, J.A. Fernandezbaca, T. Vogt, Chem. Mater. 7 (1995) 75–83.
[22] EU Research Project "*Funfluos*", NMP3-CT-2004-505575, Activity report, October 31, 2005, p. 18.
[23] M. Feist, I.K. Murwani, E. Kemnitz, J. Therm. Anal. Calorim. 72 (2003) 75.
[24] M. Feist, E. Kemnitz, Thermochim. Acta 446 (2006) 84.
[25] J. Hanss, A. Kalytta, A. Reller, Hyphenated Techniques in Thermal Analysis, in: Proc. 5th Selber Kopplungstage, E. Kapsch, M. Hollering (eds.), Bad Orb, Germany, May 25–28, 2003, pp. 151–63.
[26] E. Post, et al., Coupling techniques in thermal analysis, in: Proc. 4th Selber Kopplungstage, Selb, Germany, June 24–26, 2001.
[27] J. Ravez, A. Mogus-Milankovic, J.-P. Chaminade, P. Hagenmuller, Mater. Res. Bull. 19 (1984) 1311.
[28] V. Quaschning, J. Deutsch, P. Druska, H.J. Niclas, E. Kemnitz, J. Catal. 177 (1998) 164.
[29] R.B. King (Ed.), Encyclopedia of Inorganic Chemistry, vol. III, 2nd edn., Wiley & Sons, Chichester, 2005, p. 1540.
[30] V. Luca, C.S. Griffith, J.V. Hanna, Inorg. Chem. 48 (2009) 5663–5676.
[31] A.J. Lecloux, Texture of catalysts, in: J.R. Anderson, M. Boudart (Eds.), Catalysis—Science and Technology, vol. 2, Akademie-Verlag, Berlin, 1983, pp. 171–230.